

SEM OBSERVATIONS ON WEAR MECHANISM OF TiN-COATED HSS TWIST DRILLS WHEN DRILLING MILD STEEL

R. J. TALIB¹, S. SAAD², M. R. M. TOFF³ & A. H. HASHIM⁴

Abstract. In this study, High Speed Steel (HSS) twist drills were investigated for mechanical wear by performing drilling test on the work piece of mild steel plate. TiN coatings onto the HSS twist drills were achieved by employing reactive radio frequency (r.f) magnetron sputtering technique, which was developed in-house. The drilling performance tests were set at a rotation speed of 1,600 rpm, feed rate of 20 mm/min, and depth of cut of 25 mm. The morphological changes of the wear surface were observed using Scanning Electron Microscopy (SEM). Results of morphological examination showed that the failure mechanisms in operation during drilling were found to be adhesive and thermal wear mechanism. This paper will also discuss explicitly the processes of adhesive and thermal wear mechanism generated during drilling of twist drill on mild steel plate. Results of drilling performance test showed that the TiN coating deposited on the HSS twist drill had improved drill life by more than 2 times as compared with uncoated drill.

Keywords: HSS drill, SEM, wear mechanism, adhesive, thermal

Abstrak. Dalam kajian ini, haus mekanikal Keluli Laju Tinggi (KLT) telah dikaji dengan menjalankan ujian prestasi gerudi ke atas bahan kerja diperbuat daripada keluli lembut. Salutan TiN ke atas *HSS twist drills* diperolehi dengan menggunakan kaedah bertindak balas frekuensi radio pemercitan magnetron yang mana dibangunkan secara dalaman. Ujian prestasi gerudi dijalankan pada kelajuan pusingan 1,600 psm, kadar suapan 20 mm/minit dengan kedalaman penggerudian 25 mm. Perubahan morfologi permukaan haus diperhatikan dengan menggunakan kaedah Kemikroskopan Imbasan Elektron (KEI). Keputusan morfologi menunjukkan mekanisme rekatan dan haba beroperasi semasa proses penggerudian. Kertas kerja ini juga akan membincangkan secara mendalam proses penjanaan mekanisme haus rekatan dan haba semasa penggerudian gerudi piuhan ke atas plat keluli lembut. Keputusan ujian prestasi gerudi menunjukkan salutan TiN terendap ke atas KLT gerudi piuhan telah meningkatkan umur gerudi melebihi dua kali ganda jika dibandingkan dengan gerudi yang tidak bersalut.

Kata kunci: Gerudi KLT, KEI, mekanisme haus, rekatan, haba

1.0 INTRODUCTION

Hard coatings typically reduce the friction coefficient between drill and workpiece, thus reducing temperature during drilling process. TiN coating reduces the friction coefficient by 0.2 with the pair of TiN coating and high-speed steel, in comparison with the pair of high-speed steel [1]. Sedlacek [2] deduced that good TiN coating

¹⁻⁴ Advanced Materials Research Centre (AMREC), SIRIM Bhd., Lot 34, Jalan Hi-Tech 2/4, Kulim Hi-Tech Park, 09000 Kulim, Malaysia. E-mail: talibria@sirim.my

could produce microhardness of between 2000 to 2500 HVM. This phenomena could increase the cutting tool life. In his study on twist drills with 2 to 3 μm thick plasma assisted chemical vapour deposition (PACVD) coated thin layer, Shinzi *et al.* [3] found on average an eight-fold lifetime increase of coated twist drill, compared with uncoated drills when drilling steel plate GCr15 (1%C, 0.3%Mn, 0.25%Si, 1.45%Cr).

In earlier study, Vogel [4] reported that the main wear did not occur on the primary flank but on the lip and margin, and this result had improved on the drilling performance of unalloyed carbon, case hardened, and tool steel. In another study, Chen *et al.* [5] observed that the tool wear was due to normal mechanical abrasion and no peeling mechanism occurred on the rake, and flute surfaces of the drill. In this study, Chen *et al.* [5] used a solid board of 15% vol SiC particle reinforced Al matrix composite material as the drilling work piece. Heat generated during drilling caused cutting tools to be subjected to high temperature and resulted in thermoinstability to occur at the contact point. This phenomenon results in the generation of thermal microcracks. During machining, the temperature of between 960 – 1000°C is required in order to change the chip from original shiny steel to dark blue chips [6]. At this temperature, diffusion and oxidation process may occur at the worn area of the cutting tool [7]. Ghani *et al.* [6] also observed the generation of thermal fatigue crack on the substrate due to the phenomena of thermal cycling, coupled with thermal shock during machining.

Generally, the material surface is rough on microscopic scale with peak, and valley. The real contact point is known as the junction. In the process of sliding, the contact at the asperities causes the formation of the junction at the contact. Repeated contact can result in the formation of plastic deformation at the peak asperities, and finally causing the material to be unstable to the local shear. This phenomenon results in the process of material transfers to the opposite mating surface. The formation of transfer layers on the friction material was due to the compaction of wear debris, and a newly transferred fragment during braking [8]. The adhesion of sliding materials depends on the surface characteristic and cleanliness, surface energy, contact condition, load distribution, and suitability of the mating materials [9]. When the shearing action overcomes the cohesive bond strength of the film, the film will split and adhere to both sliding surfaces [10]. After some sliding, some of the mixed transfer layers will fall out as wear debris, but most of which will remain as a transfer film [11].

Surface temperature will be high at the contact area during sliding, and this causes the local area to expand [12]. The higher thermal expansion produces higher pressure and temperature in that region, and may result in more localised thermal expansion [13]. Expansion of the hot region to more than the surrounding area leads to the generation of compressive stress, which may cause plastic deformation on the hot region. This phenomenon may result in tensile stresses on cooling. Repeated event of such thermoinstability may result in microcrack initiation and propagation. In

another study, Kennedy [14] reported that temperature rise at the contact area introduced thermal stresses, which could superimpose onto the mechanical stresses. This phenomenon causes increased total contact stresses, thus resulting in the generation of thermomicro-cracks. As sliding progresses, thermomicrocrack growth and propagation produces multi thermomicrocracks [15].

In this study, the worn surface areas of the drill were investigated using a scanning electron microscope (SEM) to reveal the wear mechanism operated during drilling process. Based on this observation, the wear mechanism operated during drilling operation will be made.

2.0 EXPERIMENTAL TECHNIQUES

HSS twist drills were coated with a compound of TiN coating using a radio frequency (r.f) magnetron sputtering system developed by Advanced Materials Centre (AMREC), SIRIM Bhd, Malaysia, as depicted in Figure 1. The cylindrical reaction chamber is made of a stainless steel cylinder with a diameter of 500 mm, and, height of 450 mm. The negative terminal is connected to the work piece holder, which forms as the cathode. The anode and reaction chamber wall are grounded. A rotary mechanical pump is used and the chamber can be evacuated to 10^{-5} mTorr.

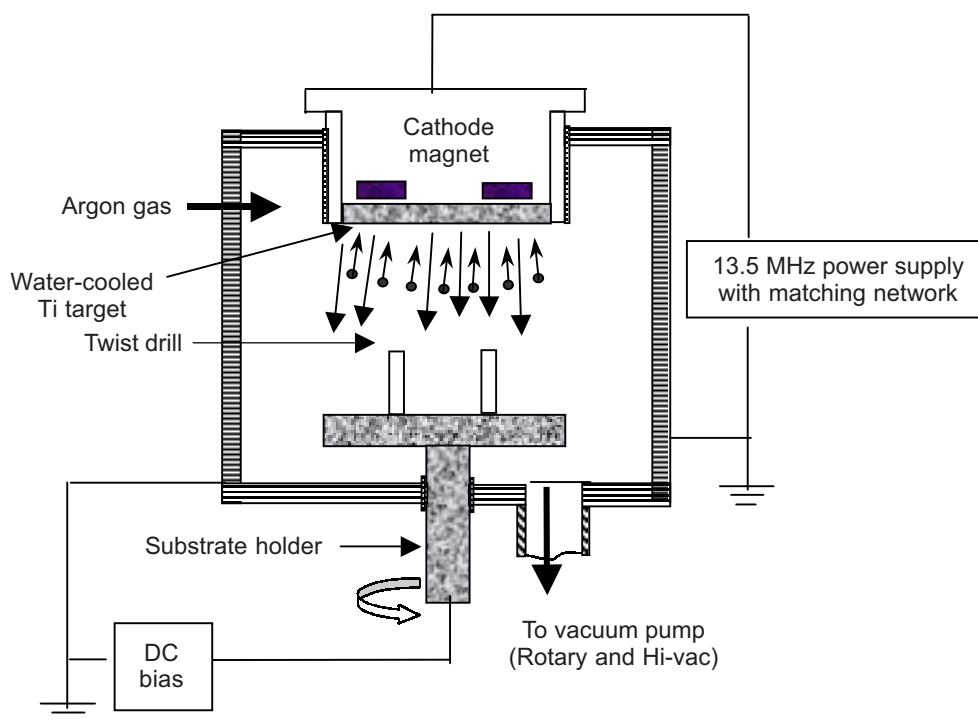


Figure 1 Schematic diagram of a radio frequency planar magnetron

Titanium with a purity of 99.9% was used as a target and placed on top of the machine. Whereas, the HSS twist drill was positioned on the substrate holder that was located at the bottom part of the machine. The distance between the titanium target and the substrate was kept constant throughout the deposition processes, at a distance of 140 mm. Prior to the deposition process, the substrates were ultra-sonic cleaned for 300 seconds. The substrates were plasma-cleaned using RF power of 200 watt for 300 seconds so that contamination was removed, and coating nucleation can be generated on the substrate surface. In this study, high purity argon and nitrogen were used as plasma and reactive gases respectively. The argon and nitrogen flow rate were fixed at 50 sccm and 10 sccm, respectively. The N₂ flow was automatically controlled by piezo-valve, driven by a logic controller according to a preset flow rate. Other coating parameters are as follows:

Substrate bias	50 Volts
Substrate temperature	50°C
Reaction pressure	8 mTorr
Deposition time	15 minutes

After being coated with TiN coating, the substrates were subjected to a drilling test to evaluate the performance of the coated drill, as compared with the uncoated HSS drill. The surface morphological changes and Energy Dispersive X-ray Analysis (EDAX) on the drill bit were observed and analysed using Scanning Electron Microscopy of model LEO 1525. The reduction of margin diameter due to wear after the drilling performance tests was measured using an optical microscope. The depth profiling on the drill was performed using X-ray Photoelectron Spectrometer, Model Jeol JPS-9200. Drilling tests were performed on a 30 mm thick mild steel plate (0.14%C, 0.61%Mn, 0.02%P, 0.01%S, 99.22%Fe and hardness of 105 HB) using CNC milling machine. The number of holes that the drills can produce was counted as the drill life. The drill life was determined at the point when the drill was unable to penetrate into the workpiece during the drilling performance tests. In this study, lubrication was not used to accelerate the wear process during the drilling experiment. The drilling test conditions are as follows:

Drill diameter	5 mm
Spindle speed	1,600 rpm
Blind hole depth of drilling	25 mm
Feed rate	20 mm/min

3.0 RESULTS AND DISCUSSION

3.1 Drilling Tests

TiN coating is gold in colour and when the drill changes to shiny colour, it indicates that the coating has wear-off. In this study, the appearance of the drill still remained gold in colour even after the 10th drilling hole, thus indicating that TiN coating was still intact on the substrate surface. The drilling performance of the coated drill has improved as compared with uncoated drill. The number of a drilling holes produced by a TiN-coated drill was about 25 holes as compared with only 12 holes produced by an uncoated drill. This shows that the tool life of a coated drill was improved by more than 2 times as compared with the uncoated drill. It was revealed that the reduction margin diameter after the 10th hole for uncoated drill was 2.49 times more than a coated drill (Table 2). The margin diameter of the drill was measured on a major tool flank with the bigger diameter, as shown in Figure 2. Thus, it could be concluded that the TiN coating did played an important role in improving the tool life of the twist drill. This phenomenon was due to the increase in microhardness, reduction in friction coefficient, and smoother surface roughness. After the 25th drilling hole, the colour of the coated drill changed to bluish colour, showing that the TiN coating had wear-off during the drilling process (Figure 2c). EDAX analysis shows that the worn surface of the coated drill did not composed of titanium and

Table 2 Reduction in margin diameter

	Margin diameter (mm)		Reduction in margin diameter (mm)
	Before	10 th holes	
Uncoated drill	5.450	5.248	0.202
TiN coated drill	5.457	5.376	0.081

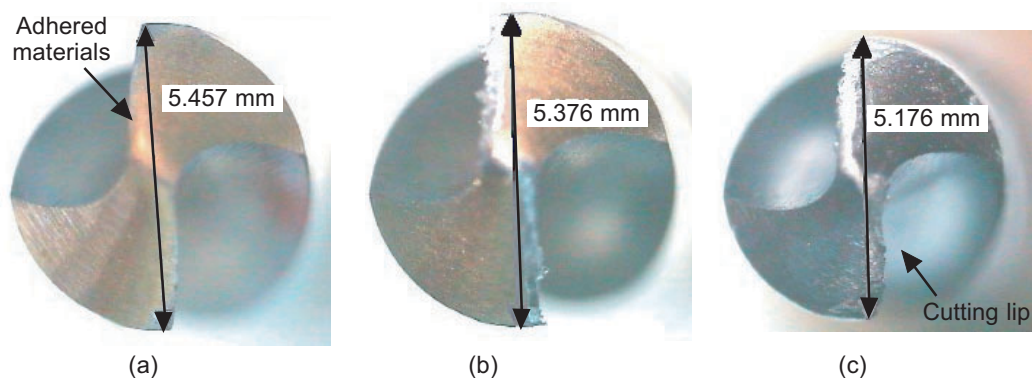
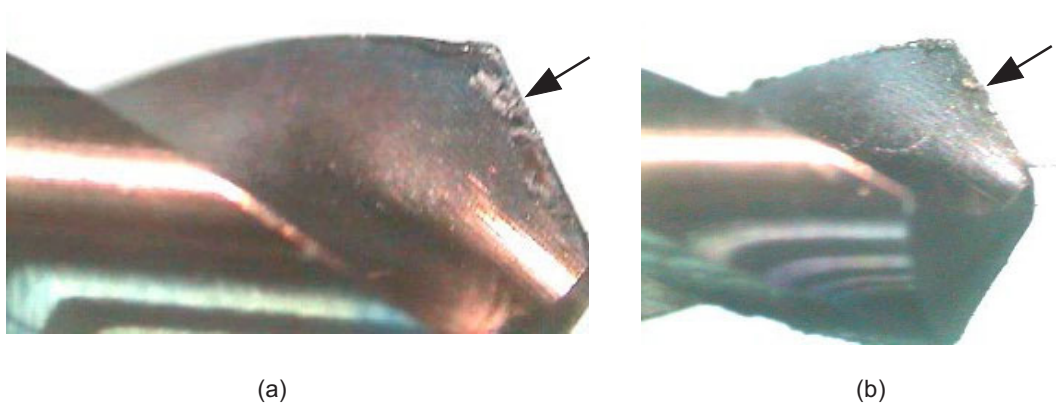


Figure 2 Margin diameter of the coated drill reduces as the number of drilling holes increased (a) before the drilling test, (b) after the 10th drilling hole, and (c) after the 25th drilling hole

Table 1 EDAX results on the worn surface of a TiN-coated drill

Element	Weight percentage (%)	
	Spectrum 1	Spectrum 2
C K	8.21	15.85
O K	3.47	13.18
V K	1.46	1.01
Cr K	3.84	2.38
Fe K	78.71	64.12
Mo K	–	3.46
W M	4.33	–
Totals	100.00	100.00

**Figure 3** Arrow sign showing chip adhered on the cutting lip of the coated drill: (a) after the 10th drilling hole, and (b) after the 16th drilling hole

nitrogen element, which have been disposed during drilling (Table 1). This bluish colour also indicates that the drill had been subjected to high temperature [6].

3.2 Wear Mechanism

The optical microscope examinations showed that the transferred material adhered to the cutting lip and chisel edge, as shown in Figures 2 and 3. It was observed that the cutting action only took place at the cutting lip. The microstructure of the uncoated HSS twist drill shows a distribution of granular metallic carbide (MC) in the matrix (Figure 4). EDAX analysis shows that the substrate materials are composed of Fe, C, V, Cr, Mo, and W, and the work piece materials are composed of Fe, C, Mn, P, and S. In the early stage of drilling (5th hole), microstructural examinations revealed that the peak asperities of the coated drill were deformed and had started to form metallic junctions as well as grow (Figure 5). With subsequent drilling, the flaking of materials occurred on the worn surface of the drill tip (Figure 6). Then, the two-way transfer

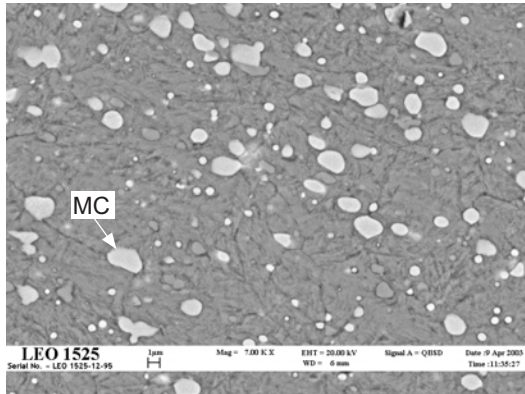


Figure 4 Distribution of metallic carbide (MC) in the matrix

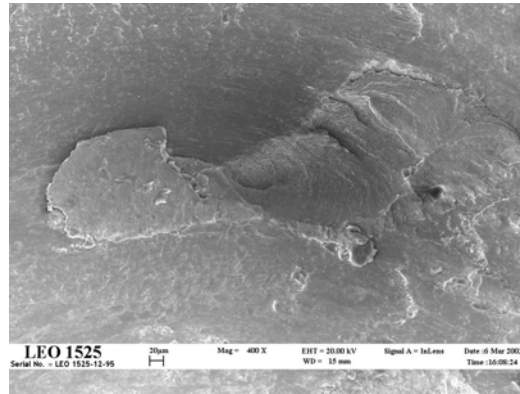


Figure 5 SEM observation on the chisel edge

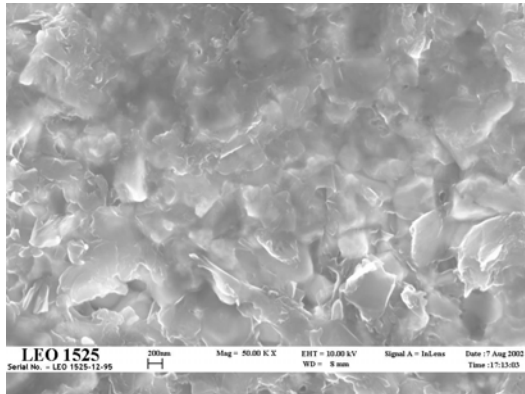


Figure 6 Flaking of materials

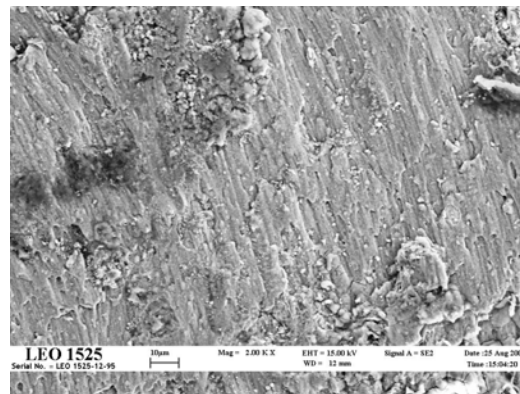


Figure 7 Generation of transfer layer on the worn surface

during sliding caused the formation of transfer layers on both sides of the sliding surfaces, as observed elsewhere [15-17]. As drilling process progressed, the transfer materials will be smeared and sheared on the worn surface of the drill (Figure 7).

This process was manifestations of adhesion wear mechanisms. The transfer films were continuously smeared and sheared on the sliding surfaces as the drilling progressed, and finally formed multilayers (Figure 8). Energy Dispersive Analysis of X-Ray (EDAX) revealed that the transfer layers generated on the worn surface contain both materials from the coated drill and the workpiece (Table 2). The materials deposited on the worn areas were found to be Ti, W, Mo, Cr, V, C, Fe, Mn, P, and S, which were materials composed in the coated drill and the workpiece. This process was due to the process of mechanical alloying on transfer layers, a phenomenon observed by other researchers such as Chen & Rigney [15,18]. Figure 9 shows that the edge of cutting lip was broken after the 25th hole and this was thought as the reason why the coated drill was unable to penetrate further into the workpiece.

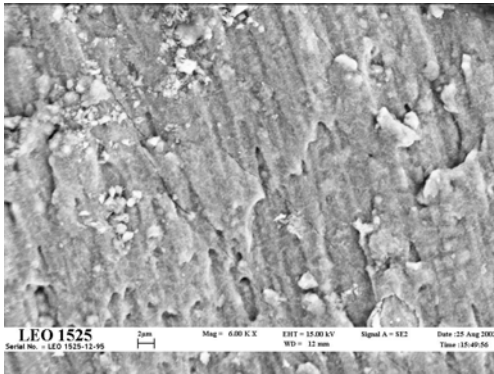


Figure 8 Micrograph shows transfer layers were smeared and sheared, and finally formed multiple layers

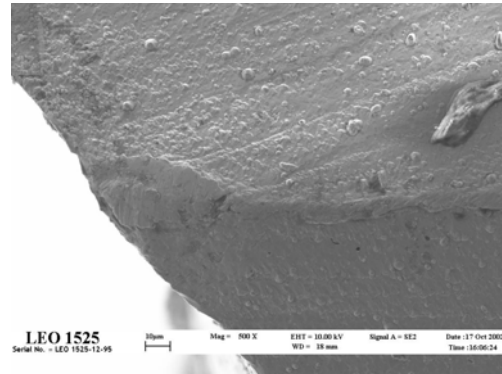


Figure 9 Broken edge at the corner of the cutting lip

Table 2 Element composition on the worn surfaces of TiN-coated drill

Element	Weight %	
	Spectrum 1	Spectrum 2
C K	28.78	21.20
O K	13.94	16.17
Si K	2.33	1.32
S K	0.32	–
V K	0.99	1.88
Cr K	1.79	1.21
Ti K	2.34	0.76
Mn K	1.91	1.91
P K	2.12	3.14
Fe K	41.2	51.23
Mo K	2.45	1.02
W M	1.83	0.93
Totals	100.00	100.00

Heat generated in the drilling operation is slightly higher than other machining processes. This is due to difficulty in delivery of cutting fluid through the flutes as the chips are flowing in the opposite direction, thus resulting in high temperature on the contact areas. As the temperature increased, some of the metal elements composed on the drill started to melt, and formed metal droplets on the interface of the sliding surfaces. With subsequent drilling, these metal droplets rolled between the two sliding surfaces and finally formed granule shapes of metal particles. As drilling continued, the granules were compacted and smeared on the worn surface. In the early stage of drilling, it was observed that the melted materials started to flow in a wavy form (Figure 10). At the same time, it was also observed that some droplets of melted

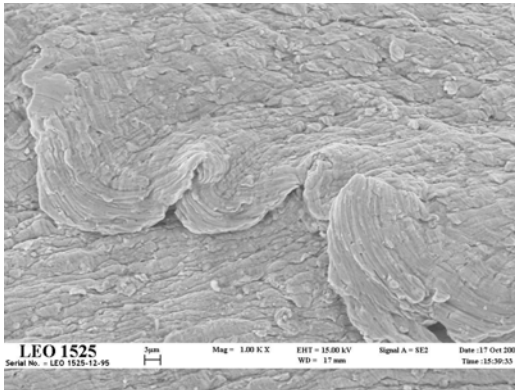


Figure 10 Material flow due to high temperature generated during dry drilling

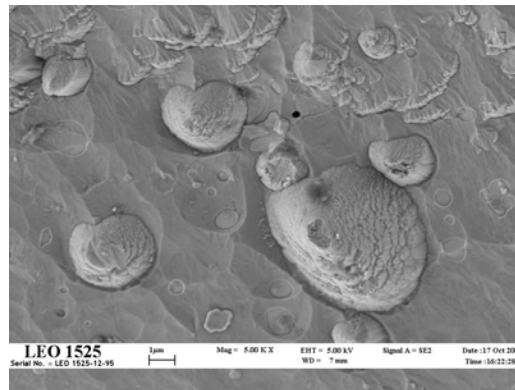


Figure 11 Formation of melted droplet on the worn surface due to high temperature

Table 3 Element composition of the droplet of melted material form on the worn surface

Element	Weight %	
	Spectrum 1	Spectrum 2
C K	4.98	7.08
O K	40.12	3.53
Ti K	31.31	–
Fe K	23.59	86.66
W M	–	2.73
Totals	100.00	100.00

material formed on the worn surface (Figure 11). EDAX on this site was composed of elements both from the drill and the workpiece, such as Fe, W, and Ti (Table 3). The materials found in this area are of high melting temperatures, whereas materials of lower melting point were not detected. This shows that the other materials in the composition, which have low melting temperatures such as Mn and P, were melted and vaporised to the atmosphere. Talib *et al.* [8] also observed the same phenomena on the worn surface of the automotive friction materials during braking process.

Thermomicrocracks were generated due to mechanical thermoinstability, as a result of high temperature. It was observed that the contact areas were located at a higher position on the wear surfaces, and thus became the contact area, as the sliding progressed (Figure 10). As drilling progressed, these contact areas formed the contact area, which would be subjected to high pressures as they have to carry high loads. At the same time, the temperature rise at the contact area introduced thermal stresses, which could superimpose onto the mechanical stresses. This phenomenon resulted in the increase of the total contact stresses. These repeated

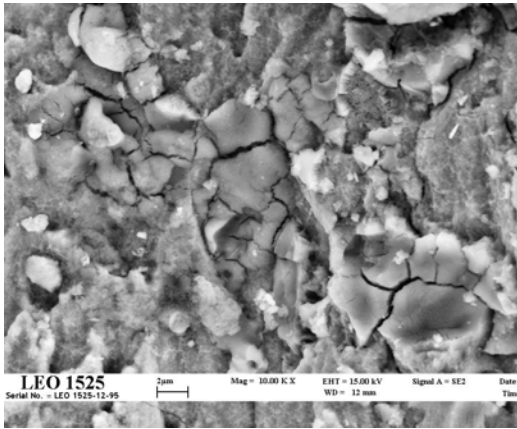


Figure 12 Early stage of thermomicrocracks generation on the worn surface of the uncoated drill

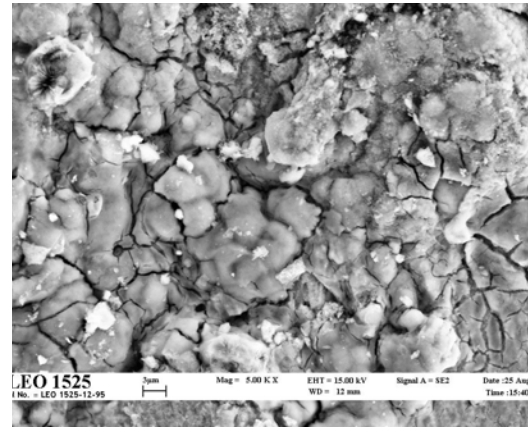


Figure 13 Generation of multi thermomicrocracks as the drilling progressed for the uncoated drill

phenomena during drilling caused the generation of thermomicrocracks at the contact areas. In the early stage of drilling, thermomicrocracks were generated at a few locations (Figure 12). With subsequent drilling, the microcracks grew, propagated, and finally joined together, forming multiple thermomicrocracks (Figure 13). After reaching a critical length, the wear particles will be disposed through the drill flutes.

There was a possibility that abrasion mechanism did operated in the early stage of drilling tests. Unfortunately, the microstructural examinations were only observed after the 10th hole, where the worn surface has been covered with transferred layers. As drilling proceeded, the peak asperities produced due to ploughing were sheared and became blunt, and the wear surfaces were covered with transfer layers, which had been compacted, smeared, and sheared.

3.3 Depth Profiling

X-ray photoelectron spectroscopy (XPS) analysis on the depth profiling of the coated sample is shown in Figure 14. It shows that the thickness of the coating was about 0.13 μm . This thickness was too thin for the TiN coating to improve significantly the hardness and wear resistance of the coated drill.

4.0 CONCLUSION

In this study, it was observed that the wear mechanism operated during drilling was a complex mixture of adhesive and thermal wears. It was also revealed that the two-way transfer of materials did occurred during the drilling process. As drilling progressed, the transfer layers were compacted, smeared, and sheared on the worn surface, whereas, the high temperature generated during drilling caused some of

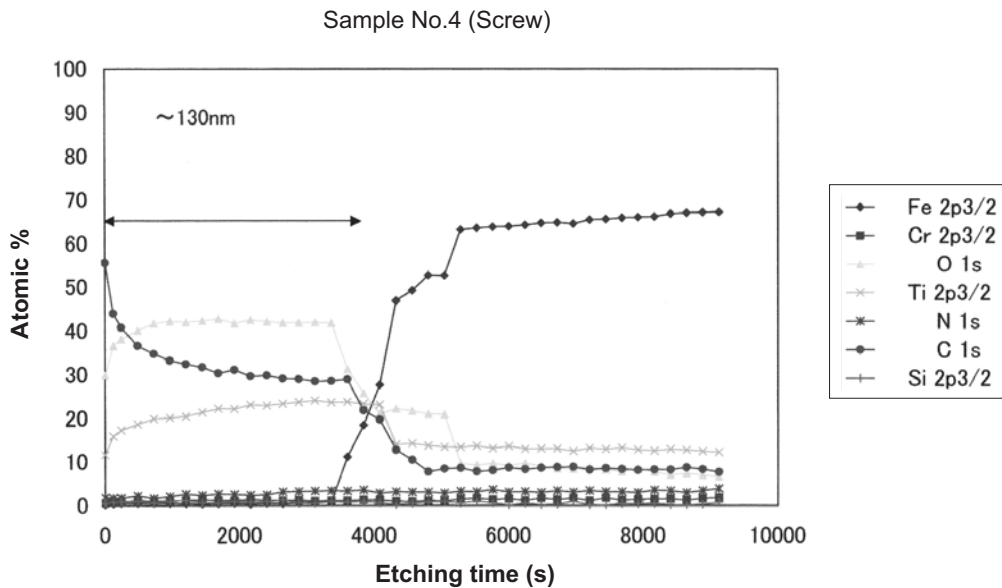


Figure 14 Depth profiling of the coated drill

the materials composed in the drill started to melt, and vaporise into the atmosphere. This phenomenon caused thermoinstability at the contact areas, and subsequently generated thermomicrocracks on the worn surface. Results of drill tests showed that a coated HSS drill had longer tool life as compared with an uncoated drill, and the main wear during drilling occurred on the cutting lip, and the margin diameter.

In this study, microhardness was found to increase from 694 to 995 HV with an increased of 43.3%, as compared with uncoated drill. Good quality coating should have the coating thickness in the range of between 2 to 15 μm [19] with a microhardness of between 2000 to 2500 HV [2], and the tool life of eight times longer [3]. This analysis shows that the developed TiN-coated drill had no significant improvement in mechanical properties as compared with commercially TiN-coated drills. Therefore, some modifications need to be done on this newly developed r.f magnetron sputtering machine, in order to get similar or better results as compared with the commercial drills.

ACKNOWLEDGEMENTS

The authors are grateful to the Government of Malaysia for funding this research project through IRPA grants 05-09-0101-0012. The assistance from the staff of the Center for Engineering Excellence, International University Islam of Malaysia, especially Mr. Mohd. Sebri for performing drilling tests, and JOEL Ltd. of Japan, especially Dr. Yoshitoki Iijima for performing XPS analysis on TiN-coated twist drills, are highly appreciated.

REFERENCES

- [1] Talib, R. J., S. Saad, M. R. M. Toff, A. H. Hashim, M. Z. Abdullah, S. Afandi, and M. A. Rahman. 2003. Tribological Properties of TiN Coating on High Speed Steel Twist Drills. *Proceeding Conference on Advanced Materials*. Putra Jaya. 22-23 May 2003.
- [2] Sedlacek, V. 1982. *Metallic Surfaces, Films, and Coatings*. Czechoslovakia: Elsevier.
- [3] Shizhi, L., Z. Cheng, X. Xiang, S. Yulong, Y. Hongshun, X. Yan, and H. Wu. 1990. The Application of Hard Coatings Produced by Plasma Assisted Chemical Vapour Deposition. *J. Surface and Coating Technology*. 43/44: 1007-1014.
- [4] Vogel, J. 1989. Ion Plating Processes of Wear-resistant Coating on Tools. In *Wear and Corrosion Resistant Coatings by CVD and PVD*. Pulkner, H. K. (ed). Chichester, U.K: Ellis Horwood Ltd. 165-196.
- [5] Chen, M., X. G. Jian, F. H. Sun, B. Hu, and X. S. Liu. 2002. Development of Diamond-Coated Drills, and Their Cutting Performance. *Journal of Material Processing Technology*. 129: 81-85.
- [6] Ning, Y., M. Rahman, and Y. S. Wong. 2001. Investigation of Chip Formation in High Speed End Milling. *Journal of Materials Processing Technology*. 113: 360-367.
- [7] Ghani, J. A., I. A. Choudhury, and H. H. Hassan. 2002. Study of Wear Mechanism of P10 TiN Coated Carbide Tools Using SEM Technique. Proc. 12th Scientific Conference Electron Microscopy Society Malaysia. Johor Bharu. 54-58.
- [8] Talib, R. J., A. Muchtar, and C. H. Azhari. 2003. Microstructural Characteristics on the Surface and Subsurface of Semi-metallic Automotive Friction Materials During Braking Process. *Journal of Material Processing Technology*. 140: 694-699.
- [9] Akagaki, T., and D. A. Rigney. 1991. Sliding Friction and Wear of Metals in Vacuum. In Ludema, K. C., and Bayer, R. G. (ed.). *Wear of Materials*. New York: American Society of Mechanical Engineers. 265-275.
- [10] Siwei, Z. 1991. Studies in Non-asbestos Friction Materials: A Brief Review. Wu, B. (ed.). *Mechanical Properties Materials Design*. Amsterdam: Elsevier Science Publisher. 403-411.
- [11] Ludema, K. C. 1992. Sliding and Adhesive Wear. In Henry, S. D. (ed.). *ASM Handbook. 18. Friction, Lubrication, and Wear Technology*. USA: American Society for Metals. 236-241.
- [12] Woodward, A. J., T. Hodges, and M. W. Moore. 1993. Advanced Measurement for Routine Assessment of Brake Performance. In Newcomb, T. P. (ed.). *Braking of Road Vehicles*. London: Institute of Mechanical Engineers. 13-21.
- [13] Barber, J. R. 1969. Thermoelastic Instabilities in the Sliding of Conforming Solids. *Proc. Royal Soc. A*. 312: 381-394.
- [14] Kennedy Jr, F. E. 1984. Thermal and Thermomechanical Effects in Dry Sliding. *Wear*. 100: 453-476.
- [15] Talib, R. J., A. Muchtar, and C. H. Azhari. 2003. A Study on Thermoinstability Process During Braking of Friction Lining Materials. Submitted to Jurnal Teknologi, UTM.
- [16] Rhee, S. K., M. G. Jacko, and P. H. S. Tsang. 1991. The Role of Friction Film in Friction, Wear, and Noise of Automotive Brakes. *Wear*. 146: 89-97.
- [17] Chen, L. H., and D. A. Rigney. 1985. Transfer During Unlubricated Sliding of Selected Metal Systems. *Wear*. 105: 47-61.
- [18] Chen, L. H., and D. A. Rigney. 1984. Wear Process in Sliding System. *Wear*. 100: 195-219.
- [19] Messier, R., A. P. Giri, and R. A. Boy. 1984. Revised Structure Zone Model for Thin Film Physical Structure. *J. Vac. Sci. Technol. A2*: 500-503.